Chapter 15
Technology of the Li-Ion Batteries

15.1 The Capacity

The irreversible capacity that is measured by the loss of capacity delivered by the battery during the first cycle (eventually also the second cycle) may have different causes. For the positive electrode, the loss of capacity during the first two cycles is often due to the fact that, when the cell is charged for the first time, the de-intercalation of lithium is accompanied with a structure modification that is not totally reversible, so that during the first discharge, some lattice distortion remains, even if the lithium can reenter into the active element of the positive electrode. As a consequence, some of the Li^+ ions will remain trapped into the particles. The irreversible capacity of $LiCoO_2$, for instance, is typically 3–5 mAh g^{-1}. Yet, this loss is relatively small, but it increases for materials that have a smaller structural stability such as $LiNiO_2$, in which case, the irreversible capacity raises up to 20–30 mAh g^{-1}. On the negative electrode side, the cause for the irreversible loss of capacity is different. In particular, for carbon-based anodes, the initial irreversibility is due to the formation of the solid-electrolyte interface (SEI) caused by the reduction of the electrolyte at the surface of the anode. The exact value of the irreversible capacity in this case depends on the shape, size and crystallinity of the carbon particles, but it remains in the range 20–30 mAh g^{-1}. Note that this part of the irreversible loss of capacity is due to the Li^+ ions that are trapped in the SEI on the anode, but these Li^+ ions have been supplied by the positive electrode during the first charge. On the other hand, Chap. 10 gives examples of situations where the initial irreversibility is huge, either because of the destruction of the crystallinity (amorphization) of the anode material during the first charge (for example: Si), or because of irreversible chemical reactions during the first discharge (for example: anodes based on alloying/de-alloying reactions). The irreversible capacity for such anodes is so large that attention is focused on the

C. Julien et al., *Lithium Batteries*, DOI 10.1007/978-3-319-19108-9_15

reversible capacity measured after the first or second cycle of the half cell, since it is the capacity that can be delivered during the life of the battery. In any case, the coulombic efficiency after the two first cycles for a battery of interest (i.e., already commercialized or under investigation in research laboratories) is close to 100 %.

15.2 Negative/Positive Capacity Ratio

The negative electrode/positive electrode ratio N/P is also called the balance of the battery. To understand the importance of this parameter, let us first consider the case of a negative electrode with initial capacity 100 mAh with irreversible capacity 10 mAh. This means that, in an experience made on a cell with this electrode and Li-metal as the counter-electrode, the measurements have shown that the formation of the SEI has consumed 10 mAh, so that the capacity delivered by the electrode after formation of the SEI is 90 mAh. For this half-cell, the formation of the SEI has no consequence, and does not limit the capacity of the half-cell, because the metal-Li is a reservoir that can provide as much of Li^+ ions as we need. This, however, is not true for the full cell. To see the effect, let us consider now the full cell with this negative electrode, and a positive electrode with an initial capacity 100 mAh and irreversible capacity 20 mAh, so that its reversible capacity is 80 mAh. During the first charge, the capacity of the positive electrode is just sufficient to allow for the formation of the SEI that consumes 10 mAh, plus fully charge the negative electrode with an amount of Li^+ ions corresponding to a capacity of 90 mAh. Upon discharging, these Li^+ ions will be delivered by the negative electrode to the positive electrode, so that only the amount of lithium inside the positive electrode now corresponds to a capacity of 100-10 = 90 mAh. However, a part of them corresponding to the irreversible capacity 20 mAh will be trapped, so that the capacity of the battery will be 90-20 = 70 mAh, while the negative electrode has a larger capacity. Therefore, the formation of the SEI has now contributed to a decrease of the reversible capacity of the full cell.

It might be tempting to increase the amount of active product in the positive electrode to increase the capacity of the battery. However, this may be not a good idea. Let us assume for instance that we increase the capacity of the positive electrode by 50 %. Then the initial capacity of the positive electrode is 150 mAh, and the irreversible capacity is 30 mAh. During the first charge, 100 mAh out of the 150 mAh available will be delivered by the positive electrode like before. Actually, if the charge is stopped at this stage, then, during the first discharge, 90 mAh will return to the negative electrode. The amount of lithium that the positive electrode can deliver in the second charge corresponds to a capacity of 140-30 = 110 mAh capacity available to proceed reversibly upon cycling, larger than the 90 mAh that the negative electrode can absorb, so that the reversible capacity is simply the reversible capacity of the negative electrode: 90 mAh. However, batteries are used usually under conditions of deep charging and discharging. In the case of the cell we have chosen, after an amount of lithium corresponding to 100 mAh have been

transferred to the negative electrode, further charging will still move the lithium remaining in the positive electrode to the negative electrode. Since, however, there is no more room for additional Li in this negative electrode, the lithium will accumulate at the surface of the negative electrode, and will thus form a Li-metal film. This effect known as lithium plating, results in a serious threat for the safety of the battery because of the possible formation of lithium oxides, so that this situation is actually prohibited. Therefore, the first criterion in the design of a battery is that the capacity of the negative electrode must be larger than the capacity of the positive electrode, despite the advantage of a gain in capacity of the battery that a larger capacity of the positive electrode might induce.

Taking this rule into account, let us see if we can increase the capacity of the initial battery we has envisioned, by increasing the capacity of the negative electrode by 50 %, instead of that of the positive electrode. Then we are left with a positive electrode with capacity 100 mAh, irreversible capacity 10 mAh, and the negative electrode now has a capacity 150 mAh, and irreversible capacity 15 mAh. Now, the same considerations as before show immediately that after the end of the first cycle, the capacity is 100-15-20 = 65 mAh instead of the initial 70 mAh when the capacity of the negative electrode was only 100 mAh. Therefore the increase of capacity of the negative electrode has actually led to a decrease of the capacity of the battery. This is due to the increase of the irreversible capacity due to the formation of the SEI that increases in the same proportion as the reversible capacity of the negative electrode, when it is obtained by simply adding active particles (same size and same shape).

Of course the example we have chosen is oversimplified: there are some degradations of the capacity upon cycling and in time, also we have assumed that the loss of irreversible capacity on the anode side was only due to the formation of the SEI supposed to be stable, and so on. It is sufficient, however, to illustrate the importance of the choice of the balance of the electrodes to determine both the safety and the capacity of the batteries.

Since the balance of the battery is a very important parameter, the battery manufacturers are usually reluctant to communicate on it. The information is released for the old-fashioned $LiCoO_2$//graphite cell that has been used for 30 years. For a standard "18650" cell (i.e., cylindrical, diameter: 18 mm, length 65 mm), the width of the anode is ~59 mm, slightly larger than the width of the cathode ~58 mm, so that the condition of a capacity of the negative electrode larger than that of the positive electrode is fulfilled, with the ratio N/P = 1.1.

15.3 Electrode Loading

The electrode loading refers to the quantity of electrode material that is deposited per unit area of the current conductor foil. This is also an important parameter that needs to be optimized. Too large loading levels introduce excessive resistance within the electrode layer and thus limits the electrical current that can cross the electrode, i.e.,

reduces the rate capability of the battery. On the other hand, decreasing the loading level increases the rate capability, but it also reduces the mass of active materials and thus the energy density. Therefore, an increased electrode area is required to compensate this reduction in order to keep the same capacity, which in turn requires a larger amount of metal foil on the current collector, and thus a mass penalty that may be larger than the reduction of the gain of mass associated with the decrease of the loading. One might wish to decrease the thickness of the metal foil to overcome this difficulty, but of course, there is a limitation imposed by the need to handle the foil during the manufacturing process of the battery. We recover here the basic conflict in Li-ion batteries between high power and high energy. Therefore, the loading level (in g cm^{-2}) is always a compromise, and its optimization is again specific to the powder that is used for the electrode, since the effective surface area also depends on the size and shape of the particles.

15.4 Degradations

The loss of capacity either with cycling (cycle life) or simply with time (calendar life) has different causes, we review in this section.

15.4.1 Damage of the Crystalline Structure

With the noticeable exception of $Li_4Ti_5O_{12}$, the active anode materials change volume when they absorb or release lithium. Upon cycling, this results in a fatigue of these active materials. In extreme cases, the result is a pulverization of the particles (see the case of Si anodes, Chap. 10). More often, like in graphite, it results in micro-cracks, exposing new parts of the particles to the electrolyte, in particular at the end of deep discharge where the variation of volume is the largest. The interaction of this new part of the active particles with the electrolyte results in the formation of additional SEI when the battery is recharged, which requires a consumption of Li, and thus a decrease of the capacity. Meanwhile the increase of the SEI leads to an increase of the resistance of the battery, and thus lowers the rate capability. In addition, this aging of the surface of the particles also results in modified electrochemical properties and thus aging of the battery.

15.4.2 Dissolution of the SEI

Traces of contaminants can be introduced in the electrolyte during manufacturing. They also can simply result from dissolved species from the positive electrode. The reason is that the positive electrode is susceptible to oxidation at the end of charge.

The dissolved species, in some cases, act as catalysts that dissolve the SEI, in particular at the end of the discharge where the SEI is less stable. To understand the consequence of such an effect on the battery, let us return to the same example similar to the one we used before, with a full cell doted with a positive electrode of initial capacity 110 mAh, irreversible capacity 10 mAh, so that its reversible capacity is 100 mAh, and a negative electrode of initial capacity 130 mAh, including an irreversible capacity 50 mAh required for the formation of the initial SEI. After the first cycle, the capacity of the cell is thus 110-10-30 = 70 mAh, smaller than the capacity 80 mAh of the negative electrode as required. Now we assume a degradation of the positive electrode so that, after 100 cycles, the SEI has been partly dissolved and the irreversible capacity associated to it has been reduced by 10 mAh. Then, if this is the only modification in the cell, the capacity after 100 cycles has increased to 80 mAh, just equal to the capacity that the negative electrode can afford, so that further degradation will result in the formation of a lithium plating at the surface of the negative electrode, just what we do not want. Of course, this is an extreme situation, but it illustrates the damage that may result from the degradation of the cathode if the resulting species dissolved in the electrolyte dissolve the SEI. It also points to the importance of choosing the couple positive-negative electrodes so that a stable SEI is formed (see Chap. 1).

15.4.3 Migration of Cathode Species

The dissolved species from the positive electrode can also migrate from the positive to the negative electrode. In this case, they can undergo reduction and produce additional surface layer. An example is the dissolution of manganese into the electrolyte in case of the $LiMn_2O_4$ spinel. As any chemical reaction, this oxidation accelerates with temperature. The experience has been made after a hot summer in the USA, where the electric cars equipped with this anode were recalled by the car maker for change of the batteries out of use. In more dramatic cases, met in particular with Ni-rich layered metal oxides, the oxygen may be released form the positive electrode, move to the carbon anode with which it will react to form CO_2.

15.4.4 Corrosion

Any residual presence of water will engender corrosion of the collectors. The lithium salt used in the Li-ion batteries is normally $LiPF_6$, which has a very good conductivity, and presents the advantage of protecting the collector in aluminum from corrosion. However, it reacts with water to form hydrofluoric acid HF that is very corrosive and thus attacks metallic collectors according to the reaction:

$$LiPF_6 + 4H_2O \rightarrow 5HF + LiF + H_3PO_4. \quad (15.1)$$

It is thus primordial to take care during the manufacturing of the battery to avoid the introduction of any trace of water.

15.5 Manufacturing and Packaging

The components of a cell are the two electrodes, the separator, and the electrolyte. The choice and role and choice of the separator have been reviewed in the chapter devoted to the safety. In this section, we review the different steps to assembly these elements in the manufacturing of the cells.

15.5.1 Step 1: Preparation of the Active Particles of the Electrodes

The synthesis of the active particles used as active elements of the electrodes, and their performance depending on the size, shape, composition, is the topic treated in the chapters devoted to anodes and cathodes. We have shown in these chapters that the active particles for both the positive and the negative electrodes are now nanoparticles. The technology of the nanoparticles is a domain in itself, and we engage the reader to read specialized books devoted to the subject [1]. We thus assume here that the step of the preparation of the active nanoparticles is achieved. In the chapters devoted to the positive and negative electrodes chapters, however, the electrodes were built with homogeneous powder since the purpose was to test the active elements and to compare their electrochemical properties. We have seen, however, that each material has its advantage and inconvenience, so that the choice depends on the application of the battery. In many applications that rely on Li-ion batteries for energy storage, the nominal duty cycle consists of a long-duration base load (typically to support ancillary or standby functions) punctuated by shorter durations of higher power demand for events such as physical actuation or communication uplink [2–4]. In the absence of electrode materials that can deliver both very high energy specific energy as well as high-rate capability, this type of power profile has led system designers to select either lower energy density systems that can support high discharge rates, or to specify dual-rate hybrid energy storage systems that use two independent storage devices: one low-rate high energy, the other high-rate low energy [5–7]. This solution leads to increased complexity at the systems level, where separate charge control electronics, packaging and wiring are needed. There is, however, another possible solution: a dual-rate hybrid battery that is based on two different active cathode materials that are incorporated into the same positive electrode structure and work in concert. The approach is not new, as there are many publications, both in the academic and patent arenas, which describe

the idea in different forms. For example, several groups have examined mixing layered $LiMO_2$ ($M = Ni, Co, Mn$) and spinel $LiMn_2O_4$ in the same cathode structure [8–10]. Other groups examined mixing $LiMO_2$ and Li_2RuO_3 in a similar fashion [11]. A use of $LiFePO_4$:$LiCoO_2$ multi-layered structure has also been proposed to increase cell tolerance to overcharge [12]. A US patent covers a broad range of possible electrode compositions and describes in detail specific cathode active material blends, including mixed $LiMO_2$ layered materials hybridized with $LiMPO_4$ materials [13]. This is a process increasingly popular for the positive electrode. For instance, the carbon-coated $LiFePO_4$ is known to be the safest cathode element, and it can deliver very high power up to 50*C* rate [14, 15]. This is thus the best cathode active element for batteries in hybrid vehicles for instance [16, 17], since this battery should be able to support a large *C*-rate upon charging to recuperate the maximum energy during the braking phase, and fast discharge during accelerations of the car. The energy density of $LiFePO_4$, however, is rather small, since the operating voltage is 3.5 V, and the capacity is 160 mAh g^{-1}. This is a limit for use in electric cars, since the driver wants the largest possible autonomy. For the lamellar compounds, it is just the opposite: they are not safe, have poor rate capability, but large capacities. In particular, the pseudo-binary system xLi$[Ni_{0.5}Mn_{0.5}]O_2$:$y$$[Li[Li_{0.33}Mn_{0.67}]O_2$ has been found to have particularly large capacities, reaching 250 mAh g^{-1} for $x = y = 0.5$, i.e., for $Li[Li_{0.17}Mn_{0.58}Ni_{0.25}]O_2$ (when charged to 4.8 V) at low *C*-rate [18–20]. Therefore, it is tempting to build a positive electrode in which both of these active elements are present to find a compromise between their advantages and disadvantages. There are three different means of preparing this electrode, shown in Fig. 15.1 [21]. The two active materials can be (a) completely mixed in a single monolithic electrode; (b) segregated into two different areas; (c) layered with the $LiFePO_4$ at the bottom, i.e., in contact with the aluminum in all these cases. The tests performed on the cells with the electrodes prepared in the three configurations have shown that it is less advantageous to mix or layer the two active elements. This is easily understood as follows. When the Li

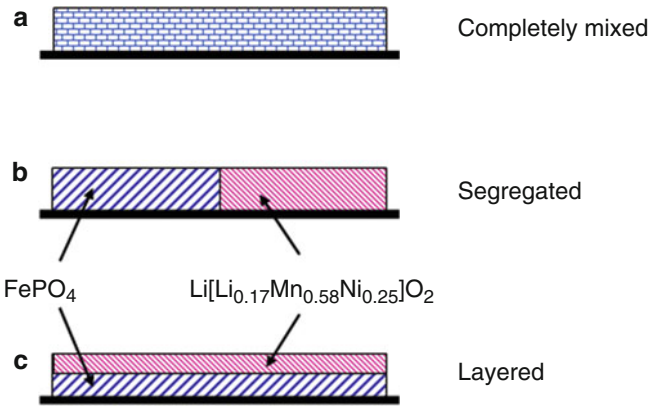

Fig. 15.1 The different means of preparing a $Li[Li_{0.17}Mn_{0.58}Ni_{0.25}]O_2$ electrode

$[Li_{0.17}Mn_{0.58}Ni_{0.25}]O_2$ and the $LiFePO_4$ are mixed intimately, all the particles are forced to be equipotential with their neighboring particles because they are in electrical contact via the high surface area conductive diluents. The consequence is an increased degree of overall electrode polarization, though the higher conductivity of the C-$LiFePO_4$ material was still able to combat severe polarization to some degree, as it likely offered a direct conductive route through the thickness of the electrode.

The layered case is more extreme: here both the electronic and the ionic conductivities of both of the constituents are manifested, as the C-$LiFePO_4$ is not present throughout the electrode to aid in electrical conductivity. All cell current is then forced to pass through the $Li[Li_{0.17}Mn_{0.58}Ni_{0.25}]O_2$ material, damming the rate capability of the electrode.

On the other hand, in the case of the physically segregated electrodes, the entire $Li[Li_{0.17}Mn_{0.58}Ni_{0.25}]O_2$ electrode can be polarized as a single body under higher discharge rates, thereby driving most current through the $LiFePO_4$ electrode. In this case, it s not requisite that all of the $Li[Li_{0.17}Mn_{0.58}Ni_{0.25}]O_2$ and $LiFePO_4$ active particles be held at the same potential within their separate electrodes.

In conclusion, mixing two active materials with disparate rate capabilities into a composite electrode is not equivalent to placing the electrodes in parallel at either an electrode or cell level. The best electrode configuration consists of segregated active materials contacting a common current collector. This arrangement allows the high-rate material to contribute fully under high current loads, without suffering the significant polarization effects associated with the low-rate material. This configuration is most similar to putting separate cells made using pure positive electrodes of the specific materials in parallel at the circuit level, a solution that is less appealing for applications requiring compact energy storage devices and simple charge control electronics. The voltage profile of the Li $[Li_{0.17}Mn_{0.58}Ni_{0.25}]O_2$—carbon coated $LiFePO_4$ in 50:50 wt% ratio built in this configuration with Li metal counter-electrode is shown in Fig. 15.2. The results were obtained by spray-deposition of the powders mixed in NMP solvent bath with 10 wt% binder and 10 wt% carbon black conductive diluents (see the next step devoted to the preparation of this laminate). The data were collected after several low-rate formation cycles were completed on the cells to encourage electrode SEI stabilization. One recognizes the voltage plateau at 3.45 V corresponding to the contribution of the $LiFePO_4$ part, to which is superposed the contribution of the Li $[Li_{0.17}Mn_{0.58}Ni_{0.25}]O_2$ component. A battery obtained by assembling such cells delivers over 700 W/kg at low rates and 300 W kg^{-1} at the rate of 3*C*.

15.5.2 Step 2: Preparation of the Electrode Laminates

The preparation is similar for both electrodes. First a conductive agent (usually carbon, acetylene black) is added to the powder in order to absorb the dilatation-contraction of the particles, and improve the electrical conductivity of the powder. Then a binder is added to plasticize the electrode, so that it can be handled.

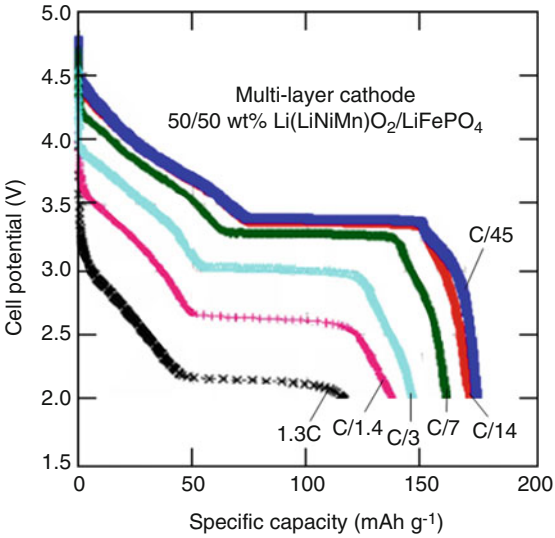

Fig. 15.2 Voltage profile of the $Li[Li_{0.17}Mn_{0.58}Ni_{0.25}]O_2$—carbon coated $LiFePO_4$ in 50:50 wt% ratio built in this configuration with Li metal counter-electrode

15.5.2.1 The Binder

The typical binder is the polyvinylidene fluoride (PVdF). In the cell manufacturing processes, *N*-methyl-2-pyrrolidone (NMP) is generally used as a solvent to dissolve the PVdF binder. Despite the widespread use of NMP, it has some disadvantages such as high cost, environmental issue associated with NMP recovery, and the severe processing control of the relative humidity (to be <2 %) to avoid the corrosion effects discussed earlier in this chapter. Also, the PVdF has strong binding strength, but low flexibility. The low flexibility can easily deteriorate cycle life characteristics of the battery due to the breaking of the bonds between active particles when important expansion/contraction process occurs during charging and discharging process. Therefore, a new trend is being developed to substitute the PVdF binder by another binder having a better elasticity to absorb the expansion and contraction stresses during cycling, in particular in anodes [22, 23]. In the case of Si-anodes, in particular, where the change of volume upon insertion or de-intercalation of lithium is very high, PVdF does not lead to good results. In such a case, the selection of a more flexible binder is very important for the electrochemical performance of anode electrodes [24–27]. So far, candidates for various new binders for Si anodes have included styrene butadiene rubber-sodium carboxymethyl cellulose (SBR-SCMC), sodium carboxymethyl cellulose (SCMC), polyamide imide (PAI), and polyacrylic acid (PAA), polyimide (PI), algae, among others [27–35] (see also Chap. 10).

Other reasons have been brought up to substitute PVdF: safety aspect of the battery, its high cost [36, 37]. Fluorine is one of the degradation products in the battery that produces stable LiF. Depending on liquid electrolytes, the formation of LiF and other harmful products with double bond ($C=CF^-$) is accelerated [38–40].

Further, self-heating thermal runaway can be induced. With respect to safety, a binder such as PVdF, which is soluble in organic solvent, is dangerous to humans and the environment. Consequently, many efforts have been done to identify suitable alternative non-fluorinated binders soluble in agent friendlier than an organic solvent. Such aqueous binders have been successfully tested and are increasingly popular for the negative electrode materials [23, 37] since some time. Their advantages are as follows: (1) low cost, (2) no pollution problem, (3) enhancement in the active material ratio in a cell owing to the reduction of binder content, (4) no requirement for strict control of the processing humidity, and (5) fast drying speed in electrode fabrication. SBR/CMC composite agent is the most popular aqueous binder, where styrene-butadiene rubber (SBR) is the primary binder, and sodium carboxymethyl cellulose (CMC) is the thickening/setting agent. Nowadays, some elastomers are commercially used as a binder for anodes in Li-ion batteries.

Recently, effort has started in the preparation of the positive electrode slurry as well [41]. However, the transition from nonaqueous to aqueous coating process has encountered some unexpected difficulties related so slurry formulation, viscosity control and film processing, which must be overcome for successful implementation in Li-ion batteries. Looking as an example the at the case of $LiFePO_4$ which is a recently commercialized positive electrode, we find that the compatibility of the elastomer binder compared to the PVdF binder, and how they connect or interact with the $LiFePO_4$ particles is different. Figure 15.3 illustrates the binding models with elastomer and PVdF binders. Regarding the CMC, it is very difficult to observe it directly in the electrode structure. We speculate that very thin CMC layer is coated at the active material of $LiFePO_4$, and some part acts as a rigid binder. During the aqueous slurry preparation process, the CMC is very important as a thickener to control the viscosity, but after coating the CMC stays almost unchanged in the electrode. CMC is an electrochemically inert part in the electrode and then eventually has no significant role in the dried electrode. We consider that the elastomer contacts quite a small surface area of each particle. This contact is enough to ensure good binding and still gives flexibility to the electrodes. The high flexibility is confirmed by the smaller electrode density when CMC is used instead of PVdF with the same active particles, and the elastomer was found to be twice

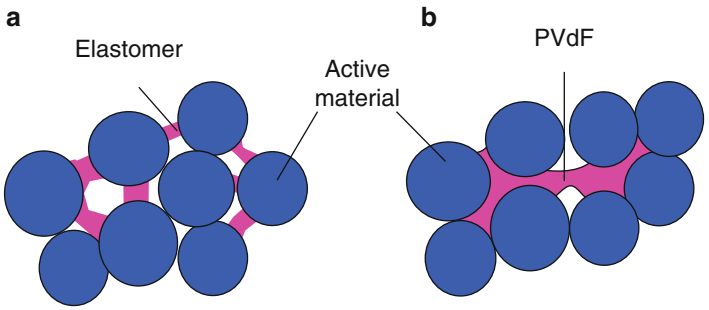

Fig. 15.3 Illustration of the binding models with (**a**) elastomer and (**b**) PVdF binder

more flexible than the PVdF [41]. Thus, the binder absorbs the expansion and the contraction of the active particles during the repeated charge and discharge since its flexibility is increased, so a battery having improved cycle life characteristics can be fabricated. In contrast, PVdF contacts a larger surface area that affects the electrode flexibility and battery cycling life. Moreover, the elastomer shows good oxidation stability up to 6 V, while PVdF shows degradation at 5.4 V. Therefore, this elastomer can be used as a binder for the next generation of 5 V-negative electrodes, while PVdF cannot be used with them, since PVdF oxidation forms a degraded fluorinated polymer, and then eventually to HF [41]. Even at the higher voltage where the elastomer degrades, the main degradation product is based on the aromatic hydrocarbon structure. This then should be the future binder not only for the negative, but also for the positive electrodes as well. However, the drawback of the aqueous suspension is the tendency of the powder to agglomerate because of the strong hydrogen bonding and electrostatic interactions [42]. Therefore, attention must be paid in implementing elastomers to control the dispersion in order to avoid the agglomeration during the preparation of the slurry. The typical mass of active materials, binder, and carbon black in dry components ranges from 75 to 90 %, 5 to 10 %, and 5 to 15 %, respectively.

15.5.2.2 Deposition on the Current Collector

The mixing of the active power, the carbon additive, and the polymer binder dissolved in a solvent is done by a planetary mixer. At the exit of the planetary mixer, the mixture that has the consistency of an ink must be deposited on the aluminum foil (positive electrode) of copper (negative electrode). This can be done by casting, coating of printing processes.

(a) *Casting*. Tape casting can be used to produce films as thin as 5 μm, while the typical thickness after drying is in the range 1.3–25 μm [43]. In this process, the slurry for the positive electrode is poured in a reservoir behind a "doctor blade" tool [44], and then cast on a moving Al foil carrier. When the slurries pass under a doctor blade, they will display a lower viscosity under the shear of the blade and a higher viscosity downstream from the blade. This prevents the slurries from spreading out of the cast region. The thickness of the wet film is given by the gap between the doctor blade and Al foil and the speed at which the Al foil moves. After the casting, the wet electrode is moved is dried so that the solvent is evaporated from the surface. At this stage, the pre-dried tape is transferred in a vacuum oven for further drying. The drying process is due to two mechanisms: evaporation of the solvent from the surface, and diffusion of the solvent through the tape to the surface. The fastest way to dry a tape is to heat the bottom of the tape without heating the air to enhance the solvent mobility in the tape, but the drying rate remains small enough so that the solvent concentration remains more or less uniform throughout the tape during the drying process.

Fig. 15.4 Image of the positive electrode formed by the deposition of the slurry onto an aluminum foil from a reservoir through a slot-die under hydraulic "pump" pressure

(b) *Coating*. The coating is quite an important process. The reader that wants more details can consult a book of 784 pages [45] devoted to the problem. Here, we simply give the basics of the process concerning the manufacturing of Li-ion batteries. Slot-die coating is another means of preparation of the negative electrodes [46]. In this process, the coating is squeezed out from a reservoir through a slot-die under hydraulic "pump" pressure onto a moving aluminum foil (Fig. 15.4). The slot is oriented perpendicular to the direction of aluminum foil movement. The success to obtain a uniform film is conditioned by the stability of the coating bead that fills the gap between the slot-die and the aluminum foil. The coating speed can be increased by applying vacuum underneath the coating bead [47]. The horizontal position of the slot-die provides the best combination of air purging at start-up and clean operation that are mandatory to make sure that the deposited film is free of any impurity. Indeed, one advantage of the slot-die method is the low contamination of the coating layer, as the entire slurry flow path is sealed against the environment until the slurry reaches the aluminum foil. Another advantage of this process is that it is contact-less because there is no doctor blade resting on the substrate, it generates no additional tensile stress in the substrate foil. Also, the coating thickness is determined by flow rate and web speed rather than gap thickness, which facilitates the obtaining of a uniform and defect-free film. The optimum operating coating parameters have been investigated in [48]. The limits of the method have been studied by Lee et al. [49]. In particular, the higher viscosity decreases the maximum operational coating speed above which the coating fails. Note this viscosity depends on the choice and concentration of the binder, but also on the size and shape of the active particles, so that it is specific to each slurry. The minimum coating thickness is also related to capillary number. One reason for the failure above the maximum speed limit is that air en entrained [50]. Air entrainment may also happen for other reasons, when the dynamic contact angle reaches 180° [50], surface roughness of the substrate [51], surface tensions of the liquid [52].

(c) *Printing*. Printing techniques (gravure or silkscreen printing, flexography) can also be used. In this case, the deposition is done by rollers covered with the ink-like slurry. After passage through a drying tunnel, the solvent has

evaporated, and a dry electrode roller is obtained. The most popular printing process is the screen printing, which is simple, highly reproducible, and efficient in large-scale production [53]. In addition no post-annealing is needed [54]. Like in the previous processes, a key issue is the obtaining of a homogeneous and stable paste with the appropriate viscosity. Also, it is important to optimize the adhesion strength between the substrate and the printed thick film. Otherwise, the film can delaminate.

A method tested on $LiCoO_2$ to increase the adhesion strength is the introduction to the slurry of a *bis*-phenol epoxy, plus dicyandiamide serving as a curing agent to remove the epoxy ring, in epoxy over dicyandiamide ratio 1/0.1 [55]. However, epoxy tended to segregate while curing and increased the surface roughness of the film. This problem could be overcome by adding ethyl cellulose resin to the paste, with a ratio of epoxy/ethyl cellulose of 1/3.

15.5.2.3 Roll Pressing Process

After deposition of the film, the strip of the electrode must be compressed, decreasing from 70 to 20–40 % the porosity, another important parameter that needs to be adjusted: the porosity must be large enough to allow for a good contact between the particles and the electrolyte, and thus a large effective surface area available for the electrochemical reactions; but is has to be small enough so that it does not impair the electrical contact between the active particles and the current collector. First, the edges of the strip are trimmed away to remove creases arising from thickness differences between coated and uncoated areas. The next step is to divide the strip lengthwise to obtain the electrode. Then, the electrode is preheated before introduction into the roll, so as to press the electrode well. A non-woven cleaning process removes impurities from the electrode surface, and finally, this electrode is wound onto a roll while maintaining tension.

15.5.3 Assembly Process

The winding process produces a jelly roll by attaching a tab to the electrode and placing the separator between the two electrodes followed by cylindrical winding. Ultrasonic welding is used to attach an aluminum and a nickel tab to the positive electrode and negative electrode, respectively. The reforming center process removes creases at the center of the jelly roll, and creates space to insert the welding tip. At this stage, the jelly roll is tested. Its electrical resistance is measured to check that it is larger than tens of MΩ. If the cell that is going to be manufactured is of cylindrical shape, the jelly roll is now ready for insertion in the can. However, when packs of many cells are required to make a battery, like in the case of electric vehicles, for instance, the cylindrical shape is not the most convenient because of

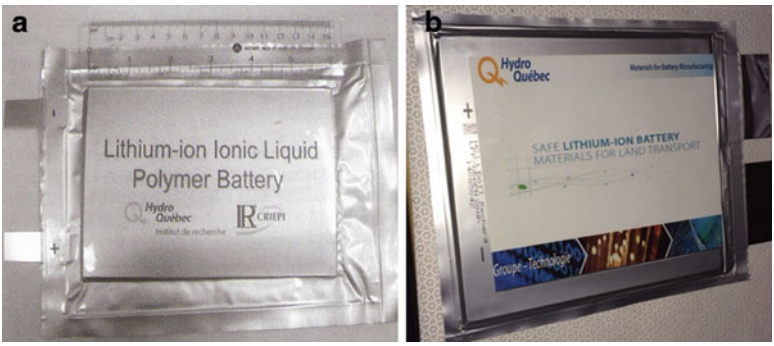

Fig. 15.5 (**a**) Li-ion flat aluminum bag cell (Ionic liquid/polymer type) with an active surface area of 104 cm^2 and (**b**) prismatic 20-Ah Li-ion cell (A4 format)

the low packing density. For this purpose, the cells are rather prepared in prismatic shape, in which case the jelly roll is pressed before insertion in the can (Fig. 15.5).

The jelly roll is inserted in the can to a certain depth that is controlled by X-ray inspection. The anode tab is bent for welding to the floor of the can. In the assembly of a cylindrical cell, the beading process creates a bent groove for the gasket to reach the top the can.

It is then time to inject the electrolyte. In the process, the internal pressure is kept lower then the atmospheric pressure, and the electrolyte is allowed to be impregnated into the jelly roll by introducing air into the can. After the electrolyte injection, electrolyte surrounding the electrode tap and beading area is wiped with a non-woven cleaning. Finally, the gasket is inserted.

The negative electrode tap welding process includes the bottom of the current break assembly. The current break is enabled by ultrasonic welding of the central area of the safety vent assembly (see Chap. 14).

The crimping process applied pressure to the top part of the battery containing the current break assembly, the positive temperature coefficient (PTC) and cap-up. After sealing the current break, the PTC, and the cap-up either soldered shut by a laser beam or into a heat-sealed soft pouch, the crimped cell is pressed to maintain a constant height. The cell is ready for inspection by X-rays to check for any defect and verify the internal assembly of all these elements. After washing with water to remove electrolyte and any impurity at the surface, the cell is dried to eliminate moisture. Finally, the battery in imprinted with the manufacturing factory, line number and date.

15.5.4 Formation Process

Since the SEI is formed during the initial charging, it is of primary importance for the future performance and the life of the battery that the first cycles to be done according to a protocol that permits the SEI to be well formed and stabilized to

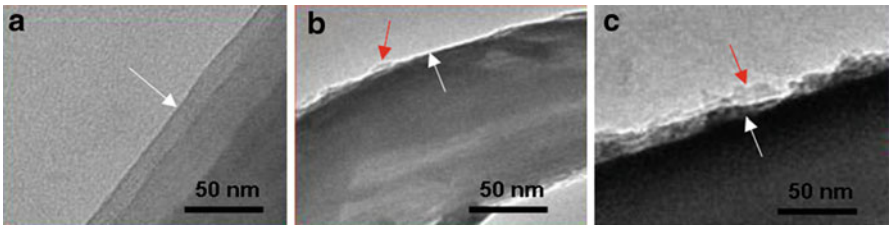

Fig. 15.6 TEM images showing the SEI formation onto the surface of graphite electrode. (**a**) Fresh electrode, (**b**) after discharge at 1.2 V and (**c**) after discharge at 0.05 V. *White* and *red arrows* indicate the edge of graphite and SEI layer, respectively

avoid decomposition of the electrolyte (Fig. 15.6). That is this formation test is made by the manufacturer, and must then be considered a part of the manufacturing process. Some of the faulty cells can also be detected during this procedure, because the main cause of failure is internal short-circuits, leading to drop in the open circuit voltage and discharge capacity. These faulty batteries are discarded, and the tolerance on the capacity is small, because when they are connected in parallel or in series inside a pack, they must have the same characteristics, and in particular the same capacity within 3 %. Therefore, when the battery has been prepared by following the previous steps described in Sects. 15.4.1–15.4.4, it is fully charged and stabilized for few hours. After elimination of any faulty cell, the fully charged cells are then kept under constant temperature and humidity for a month and controlled. Then the battery is fully discharged to check for its capacity, and the battery is classified according to its discharge capacity, one level corresponding to 3 % discharge capacity. The battery is now ready to be commercialized, and in the discharged state.

15.5.5 The Charger

The first task of the consumer after he/she has bough a battery is then to charge it. This operation is done by a charger. Inside this device, electronics protect the battery from overcharge that, by definition, occurs when too much of lithium is sent to the negative electrode. As we have seen in the section devoted to the capacity and balance between the electrode, the negative electrode, by construction, should have a capacity larger that the positive electrode. Therefore, it is not possible in principle to reach a situation where an excess of lithium coming from the positive electrode would form of lithium layer at the surface of the negative electrode. Nevertheless, overcharge results in a sharp increase in the voltage associated to the rise in the internal resistance of the battery, resulting in an increase of the internal temperature and possible thermal runaway and battery fire, because when the active particles of the positive electrode have been emptied from their lithium content,

they are insulating. In some cases, it also results in a structural collapse of the active particles of the positive electrode, with the risk of explosion. The battery charge is thus equipped with an electronic device to control carefully the charge of the battery. In case the lithium intercalation/extraction of lithium of the active particles of at least one of the two electrodes proceeds through a solid solution, the voltage of the cell depends on the charge of the cell. The control can then be made by measurements of the voltage. In case the lithium intercalation/extraction proceeds with a two-phase reaction, we have seen in Chaps. 1 and 2 that the voltage profile is a plateau; in this case, met in the new generation of batteries with $LiFePO_4$ as a cathode in particular, the control is done by measurements of the current, which, integrated over time, determines directly the amount of Li^+ ions that have been transferred to the negative electrode. In any case, the operational voltage at a given state of charge is specific to the each positive-negative electrode couple. In addition, the current that cross the battery during the charge must be controlled and limited so that the battery is not too far from thermodynamic equilibrium during the charge process, otherwise large over-potential would occur. The charger is also equipped with electronics to control the dynamics of the charge process. Usually, the charge is triggering process, in which the charge proceeds by steps, each step being defined by charging controlled by the current followed by a period of time where the battery is left at rest for equilibration. Again, the kinetics of the motion of the lithium inside the battery is specific to the choice of the electrodes. For these reasons, it is mandatory to charge the battery with the charger delivered by the constructor, i.e., the charger that has been adapted specifically to this particular battery.

References

1. Hosakawa M, Nogi K, Naito M, Yokoyama T (eds) (2008) Nanoparticles technology handbook. Elsevier, New York
2. Mayo RN, Ranganathan P (2005) Energy consumption in mobile devices: why future systems need requirements – aware energy scale-down. In: Salsafi B, Vijaykumar TN (eds) Power – aware computer systems. Lect Notes Comput Sci 3164:26–39
3. Verbrugge M, Frisch D, Koch B (2005) Adaptive energy management of electric and hybrid electric vehicles. J Electrochem Soc 152:A333–A342
4. Harrison AI (2003) The changing world of standby batteries in telecoms applications. J Power Sourc 116:232–235
5. Lam LT, Louey R (2006) Development of ultra-battery for hybrid-electric vehicle applications. J Power Sourc 158:1140–1148
6. Chandrasekaran R, Sikha G, Popov BN (2005) Capacity fade analysis of a battery/super capacitor hybrid and a battery under pulse loads – full cell studies. J Appl Electrochem 35:1005–1013
7. Han J, Park ES (2002) Direct methanol fuel-cell combined with a small back-up battery. J Power Sourc 112:477–483
8. Park SH, Kang SH, Johnson CS, Amine K, Tackeray MM (2007) Lithium-manganese-nickel-oxide electrodes with integrated layered-spinel structures for lithium batteries. Electrochem Commun 9:262–268

9. Arrebola JC, Caballero A, Hernan L, Morales J (2005) Expanding the rate capabilities of the $LiNi_{0.5}Mn_{1.5}O_4$ spinel by exploiting the synergistic effect between nano and microparticles. Electrochem Solid State Lett 8:A461–A645
10. Ma ZF, Yang XQ, Liao XZ, Sun X, McBreen J (2001) Electrochemical evaluation of composite cathodes base on blends of $LiMn_2O_4$ and $LiNi_{0.8}Co_{0.2}O_2$. Electrochem Commun 3:425–428
11. Stux AM, Swider-Lyons KE (2005) Li-ion capacity enhancement in composite blends of $LiCoO_2$ and Li_2RuO_3. J Electrochem Soc 152:A2009–A2016
12. Imachi N, Takano Y, Fujimoto H, Kida Y, Fujutani S (2007) Layered cathode for improving safety of Li-ion batteries. J Electrochem Soc 154:A412–A416
13. Barker J, Saidi MY, Tracey EK (2006) Electrodes comprising mixed active particles. US Patent 7,041,239. Accessed 9 May 2006
14. Zaghib K, Dontigny M, Guerfi A, Charest P, Rodrigues I, Mauger A, Julien CM (2011) Safe and fast-charging Li-ion battery with long shelf life for power applications. J Power Sourc 196:3949–3954
15. Zaghib K, Dontigny M, Guerfi A, Trottier J, Hamel-Paquet J, Gariepy V, Galoutov K, Hovington P, Mauger A, Groult H, Julien CM (2012) An improved high-power battery with increased thermal operating range: C–$LiFePO_4$//C–$Li_4Ti_5O_{12}$. J Power Sourc 216:192–200
16. Zaghib K, Dubé J, Dallaire A, Galoustov K, Guerfi A, Ramanathan M, Benmayza A, Prakash J, Mauger A, Julien CM (2014) Enhanced thermal safety and high power performance of carbon-coated $LiFePO_4$ olivine cathode for Li-ion batteries. J Power Sourc 219:36–44
17. Zaghib K, Dontigny M, Perret P, Guerfi A, Ramanathan M, Prakash J, Mauger A, Julien CM (2014) Electrochemical and thermal characterization of lithium titanate spinel anode in C-$LiFePO_4$//C-$Li_4Ti_5O_{12}$ cells at sub-zero temperatures. J Power Sourc 248:1050–1057
18. Wu Y, Manthiram A (2006) High capacity, surface-modified layered $Li/Li[Ni_xLi_{(1/3-2x/3)}Mn_{(2/3-x/3)}]O_2$ cathodes with low irreversible capacity loss batteries, fuel cells, and energy conversion. Electrochem Solid State Lett 9:A221–A224
19. Lu ZH, Dahn JR (2002) Understanding the anomalous capacity of $Li/Li[Ni_xLi_{(1/3-2x/3)}Mn_{(2/3-x/3)}]O_2$ cells using in situ X-ray diffraction and electrochemical studies. J Electrochem Soc 149:A815–A822
20. Lu ZH, Beaulieu LJ, Donaberger RA, Thomas CL, Dahn JR (2002) Synthesis, structure, and electrochemical behavior of $Li[Ni_xLi_{(1/3-2x/3)}Mn_{(2/3-x/3)}]O_2$. J Electrochem Soc 149:A778–A791
21. Whitacre JF, Zaghib K, West WC, Ratnakumar BV (2008) Dual active material composite cathode structures for Li-ion batteries. J Power Sourc 177:528–536
22. Fukunaga M, Suzuki K, Kuroda A (2003) The 44th battery symposium in Japan. Abst #1D19, p 462
23. Zhang SS, Xu K, Jow TR (2004) Evaluation on a water-based binder for the graphite anode of Li-ion batteries. J Power Sourc 138:226–231
24. Chen Z, Chevrier V, Christensen L, Dahn JR (2004) Design of amorphous alloy electrodes for Li-ion batteries: a big challenge. Electrochem Solid State Lett 7:A310–A314
25. Chen Z, Christensen L, Dahn JR (2003) Comparison of PVDF and PVDF-TFE-P as binders for electrode materials showing large volume changes in lithium-ion batteries. J Electrochem Soc 150:A1073–A1078
26. Chen Z, Christensen L, Dahn JR (2003) Large-volume-change electrodes for Li-ion batteries of amorphous alloy particles held by elastomeric ethers. Electrochem Commun 5:919–923
27. Liu R, Yang MH, Wu HC, Chiao SM, Wu NL (2005) Enhanced cycle life of Si anode for Li-ion batteries by using modified elastomeric binder. Electrochem Solid State Lett 8: A100–A103
28. Li J, Lewis RB, Dahn JR (2007) Sodium carboxymethyl cellulose: a potential binder for Si negative electrodes for Li-ion batteries. Electrochem Solid State Lett 10:A17–A20
29. Bridel JS, Azaïs T, Morcrette M, Tarascon JM, Larcher D (2010) Key parameters governing the reversibility of Si/carbon/CMC electrodes for Li-ion batteries. Chem Mater 22:1229–1241

30. Choi NS, Yew KH, Choi WU, Kim SS (2008) Enhanced electrochemical properties of a Si-based anode using an electrochemically active polyamide imide binder. J Power Sourc 177:590–594
31. Magasinski A, Zdyrko B, Kovalenko I, Hertzberg B, Burtovyy R, Huebner CF, Fuller TF, Luzinov I, Yushin G (2010) Toward efficient binders for Li-ion battery Si-based anodes: polyacrylic acid. ACS Appl Mater Interfaces 2:3004–3010
32. Ding N, Xu J, Yao Y, Wegner G, Lieberwirth I, Chen C (2009) Improvement of cyclability of Si as anode for Li-ion batteries. J Power Sourc 192:644–651
33. Chong J, Xun S, Zheng H, Song X, Liu G, Ridgway P, Wang JQ, Battaglia VS (2011) A comparative study of polyacrylic acid and poly(vinylidene difluoride) binders for spherical natural graphite/$LiFePO_4$ electrodes and cells. J Power Sourc 196:7707–7714
34. Kiovelko I, Zdyrko B, Magasinski A, Hertzberg B, Milicev Z, Burtovyy R, Luzinov I (2011) A major constituent of brown algae for use in high-capacity Li-ion batteries. Science 334:75–79
35. Kim JS, Choi W, Cho KY, Byun D, Lim JC, Lee JK (2014) Effect of polyimide binder on electrochemical characteristics of surface-modified silicon anode for lithium ion batteries. J Power Sourc 244:521–526
36. Lee JH, Kim JS, Kim YC, Zang DS, Paik U (2008) Dispersion properties of aqueous-based $LiFePO_4$ pastes and their electrochemical performance for lithium batteries. Ultramicroscopy 108:1256–1259
37. Lee JH, Lee S, Paik U, Choi YM (2005) Aqueous processing of natural graphite particulates for lithium-ion battery anodes and their electrochemical performance. J Power Sourc 147:249–255
38. Maleki H, Deng G, Haller IK, Anami A, Howard JN (2000) Thermal stability studies of binder materials in anodes for lithium-ion batteries. J Electrochem Soc 147:4470–4475
39. Gaberscek BM, Drofenik J, Dominiko R, Pejovnik S (2000) Improved carbon anode for lithium batteries pretreatment of carbon particles in a polyelectrolyte solution. Electrochem Solid State Lett 3:171–173
40. Oskam G, Searson PC, Jow TR (1999) Sol-gel synthesis of carbon/silica gel electrodes for lithium intercalation articles. Electrochem Solid State Lett 2:610–612
41. Guerfi A, Kaneko M, Petitclerc M, Mori M, Zaghib K (2007) $LiFePO_4$ water-soluble binder electrode for Li-ion batteries. J Power Sourc 163:1047–1052
42. Nahass P, Rhine WE, Pober RL, Bowen HK, Robbins WL (1990) A comparison of aqueous and non-aqueous slurries for tape-casting, and dimensional stability in green tapes. In: Nair KM, Pohanka R, Buchanan RC (eds) Materials and processes in microelectronic systems, ceramic transactions, vol 15. American Ceramic Society, Westerville OH, pp 355–364
43. Mistler RE, Twiname ER (2000) Tape casting: theory and practice. American Ceramic Society, Westerville, OH
44. Berni A, Mennig M, Schmidt H (2004) Sol-gel technologies for glass producers and users. Springer, New York, pp 89–92
45. Tracton AA (ed) (2005) Coatings technology handbook. CRC Press, Taylor & Francis Group, Boca Raton
46. Hodges AM, Chambers G (2005) Multilayer; dielectric substrate overcoated with electroconductive layer US Patent 6,946,067. Accessed 20 Sept 2005
47. Chang YR, Chang HM, Lin CF, Liu TJ, Wu PY (2007) Three minimum wet thickness regions of slot die coating. J Colloid Interface Sci 308:222–230
48. Chu WB, Yang JW, Wang YC, Liu TJ, Tiu C, Guo J (2006) The effect of inorganic particles on slot die coating of poly(vinyl alcohol) solutions. J Colloid Interface Sci 297:215–225
49. Lee KY, Liu LD, Ta-Jo L (1992) Minimum wet thickness in extrusion slot coating. Chem Eng Sci 47:1703–1713
50. Deryagin BV, Levi SM (1964) Film coating theory. The Focal Press, New York
51. Buonopane RA, Gutoff EB, Rimore MMT (1986) Effect of pumping tape surface properties on air entrainment velocity. AIChE J 32:682–683

52. Burley S, Kennedy BS (1976) An experimental study of air entrainment at a solid/liquid/gas interface. Chem Eng Sci 31:901–911
53. Tymecki L, Zwierkowska E, Koncki R (2004) Screen-printed reference electrodes for potentiometric measurements. Anal Chim Acta 526:3–11
54. Park MS, Hyun SH, Nam SC (2006) Preparation and characteristics of $LiCoO_2$ paste electrodes for lithium ion micro-batteries. J Electroceramics 17:651–655
55. Park MS, Hyun SH, Nam SC (2007) Mechanical and electrical properties of a $LiCoO_2$ cathode prepared by screen-printing for a lithium-ion micro-battery. Electrochim Acta 52:7895–7902